Miniature Pumped Fluid Loop Regulating Payload under Simulated Earth Albedo Heat Load on Radiator

Mikael Antelius[1], Robert Thorslund[2], Are Bjorneklett[3] and Peter Nilsson[4]
APR Technologies, Enköping, 745 39, Sweden

and

Pierre Henriot[5] and David Valentini[6]
Thales Alenia Space, Cannes, 06150, France

We present the breadboard development of a miniature pumped monophasic fluid loop designed for thermal regulation on spacecraft's in an LEO orbit. The pumped loop is completely free of moving parts where the pump technology is based on electro hydro dynamic pumping of a dielectric fluid. This pumping mechanism gives unique advantages, e.g. variable thermal conductance (regulated thermal conductivity) and high reliability. The breadboard system includes a pump, a liquid volume expansion chamber, a cold side heat exchanger, a Shapal® CTE matched to the payload hot side heat exchanger, tubing and control electronics.Thermal tests on the breadboard system shows that the system behaves as expected. A thermal resistance of 0.59K/W was measured and a capability of regulating the hot side heat exchanger to a deviation better than 0.15 °C when a simulated earth albedo heat load was applied to the radiator. Stability measurements over 24h with constant pumping power shows a stable system thermal conductance with no deviation. The total system mass is below 350g and the system consumes less than 0.3W of power.

Nomenclature

CTE	=	coefficient of thermal expansion
EHD	=	electrohydrodynamic
EM	=	engineering model
EPPL	=	european preferred parts list
LEO	=	low earth orbit
MLI	=	multilayer insulation
PID	=	proportional–integral–derivative
PWM	=	puls width modulation
TIG	=	tungsten inert gas

I. Introduction

SPACECRAFT thermal management is of utmost importance for spacecraft design and performance. In this field, pumped fluid loops systems have a wide potential application span from simple constant conduction heat transfer to closed loop thermal control. In contrast to heat pipes and thermal conduction, pumped loops require an active pump. However, by utilizing an Electrohydrodynamic (EHD) pump, moving parts, added vibration and reduced service life can be avoided. The EHD pumped loop system is particularly suited for temperature control

[1] R&D Engineer, Västra Järnvägsgatan 4, 745 39 Enköping.
[2] CTO, Västra Järnvägsgatan 4, 745 39 Enköping.
[3] CSO, Västra Järnvägsgatan 4, 745 39 Enköping.
[4] CEO, Västra Järnvägsgatan 4, 745 39 Enköping
[5] Thermal Specialist, Engineering Department, Science and Observation, 5 Allée des Gabians, 06150 Cannes.
[6] Head of Thermal section, Engineering Department, Science and Observation, 5 Allée des Gabians, 06150 Cannes.

applications. The fluid flow rate is controlled by the strength of the internal electrical field generating the EHD flow and on/off or analogue control schemes can be utilized.

Although the pump is driven by an externally applied electric field, the required energy input is low (<0.3 W), much less than typical electrical motors used in mechanically pumped fluid loops. The EHD pump technology developed and described herein is furthermore scalable across a wide range of fluid flow rates, operating temperatureranges and mechanical envelopes. In comparison with heat pipes and Loop Heat Pipes, EHD pumped fluid loops are much less affected by gravitational field, thus simplifying ground testing.

In this paper we present the breadboard development and thermal performance of a monophasic EHD pumped fluid loop designed for closed loop thermal regulation on spacecraft in LEO.

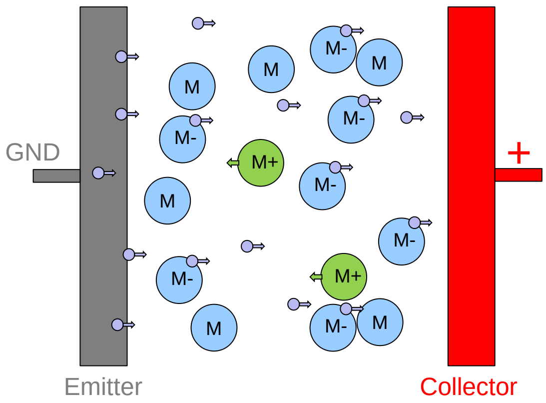

Figure 1. Ion drag pumping. *A flow between emitter and collector is created by the ion drag from accelerating ions. Using perforated electrodes, a net flow to the right is generated.*

II. EHD Pump Fundamentals

Electrohydrodynamics[1] is the study of the interaction between electrical fields and dielectric fluids. This interaction can be used to generate fluid movement[2]. The EHD pump mode utilized in this development is designated as an ion drag pump. In this pump, ions are generated by electron injection into fluid molecules at a metal/liquid interface (the electrode surface). This electron generation is facilitated by the electric field concentrations at the edges of the porous electrode. This formed ion is accelerated by an electric field towards an oppositely charged electrode, and as it travels through the liquid the ion generates an ion drag. Ion drag is basically accelerating ions that are pushing/bringing along the adjacent molecules by friction. The ions are neutralized at the destination electrode. This is the intended mode of operation, which is illustrated in Figure 1.

III. System Overview

An overview of the developed system is shown in Figure 2. The system consists of two heat exchangers connected by 2 tubes and additionally a pump and a liquid expansion chamber. The system is single-phase and the two tubes carries coolant in different directions. Photographs of all the components are shown in Figure 3. In this development the electronics has not been integrated into the pump housing. The high voltage input pins can be seen

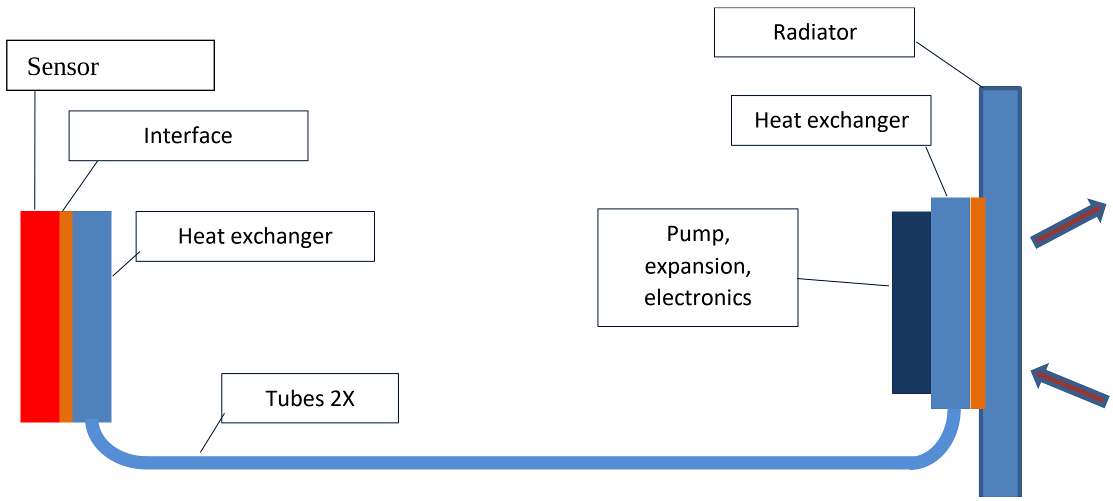

Figure 2. System overview. *The developed thermal regulation system with sensor and radiator added for clarity. The emulated sensor is simply a heater while the radiator temperature is controlled externally to emulate a LEO orbital variation in absorbed heat flux on the radiator.*

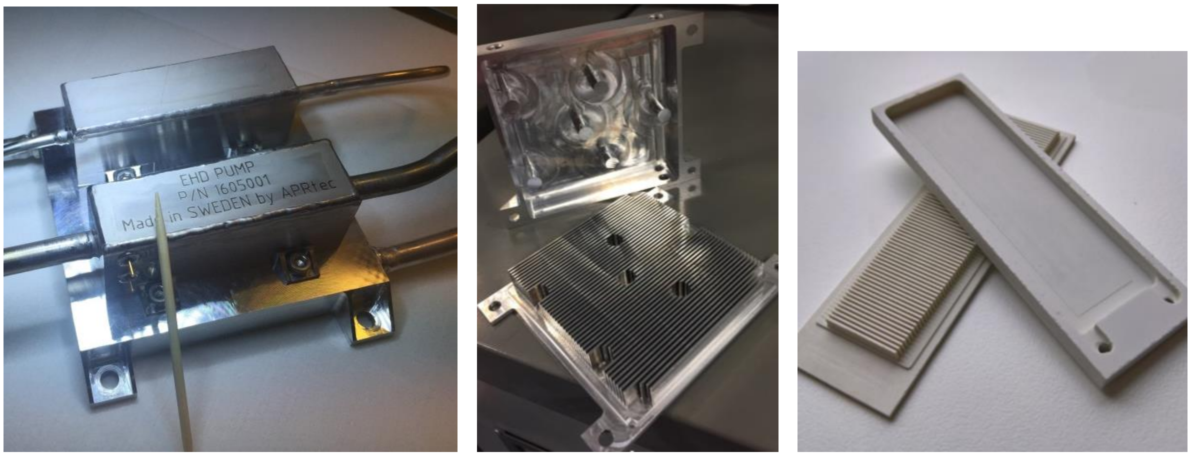

Figure 3. Left: Cold side heat exchanger assembly. *The cold side heat exchanger carries the liquid expansion chamber (top) and EHD pump (bottom). A tooth pick has been added for scale.* **Center:** *Cold aluminium heat exchanger before assembly.* **Right:** *Shapal heat exchanger before assembly.*

to the left of the tooth pick in Figure 3 Left. Integrating is however preferable due to the relatively high voltage. We have previously shown a system with such an integration[3].

A. Materials Selection

It is usually of interest and importance to keep a system as simple as possible when it comes to the selection of materials used in the system. It is also preferable to reduce the use of different materials as much as possible. The reason is that there is always a risk when mixing different materials that something unknown could occur. Thus, choosing compatible materials is of importance. Other important parameters influenced by the material choices are the manufacturability of the system, the system performance, the complexity and the final cost.

Three different materials have been evaluated; Stainless Steel 316L/316 (1.4404), Aluminum (alloy 6082/6063) and Shapal. The material choice for every component is a trade-off based on previous experience and the advantages and disadvantages presented in Table 1.

Comparing the pros and cons, Aluminum has a few great advantages over Stainless Steel and is the preferred material. The disadvantages are mainly manufacturing and assembly related. Therefore, Aluminum was used for the cold heat exchanger while stainless steel was used for the more intricately designed pump body and expansion chamber. The tubing was also in stainless steel, but for reliability reasons. The only reason to use Shapal is when CTE matching requires it, as is the case for the warm heat exchanger which is directly coupled to a ceramic electronics package.

B. Component Assembly

The tube connectors on the heat exchangers will be made of a friction stir welded 2-layer metal which creates a full fusion weld. The bimetallic interface will consist of SS316-Aluminium, the Aluminium end of the interface will

Table 1. Advantages and disadvantages of materials for the system components.

Material	Advantage	Disadvantage
Aluminium 6082/6083	Low density High thermal conductivity (heat exchangers) Fluid compatibility Machinability (less expensive)	Weldability (laser, micro tig) Assembly compatibility
Stainless steel 1.4404	Weldability (laser, micro tig) Assembly compatibility Fluid compatibility	Density Low thermal conductivity (heat exchangers) Machinability (more expensive)
Shapal Hi-M Soft AlN-BN ceramic	Low density CTE matched to silicon and ceramic packages High thermal conductivity (heat exchangers) Fluid compatibility	Machinability (more expensive) Assembly compatibility

be vacuum brazed to the heat exchanger, at the same time as the heat exchanger bottoms and lids are joined. The SS316 end connector will allow for a solid TIG welding process of the tubes to the heat exchangers. The other stainless steel parts are also TIG welded together.

The pump core is located inside the pump housing and it consists of a glazed ceramic-metal assembly. The pump core is assembled from alternating layers of ceramic spacers and porous, microstructured and metal-coated electrodes. Many of these ceramic and electrode components form an array of electrode pairs, which are energized by a single custom made EHD power supply.

The pump body is the only part of the liquid filled system that needs feed-throughs. These feed-throughs connect the pumpcore inside the housing. The selected component are micro-TIG welded to the housing and has a compression glass insulated gold-plated NiFe (alloy 48) pin.

C. Coolant

APRtec's EHD pump can pump all types of dielectric liquids and gases, but the performance vill vary greatly depending on the properties of the fluid. In this project we use the Novec engineered fluids from 3M that have good properties both for the EHD pump functionality and for heat transfer applications. Some of the desired parameters are high heat carrying capacity, low viscosity, low coefficient of expansion and high dielectric constant. To be able to reach the required flowrates with a compact pump and for the best system performance we has chosen Novec 7200 as the fluid. This fluid has the best properties overall, and most importantly, the viscosity is low, which greatly reduces the flow resistance. A possible weakness for this liquid is the low boiling point of 76 °C. But, the boiling point for the Novec fluid will be elevated by *roughly* 15-20 °C/atm of internal pressure.

Table 2. Specification overview. *The requirements of the EM system compared to the performance/characteristics of the manufactured EM.*

Characteristic	Requirement
Heat load	3 W @ -22 °C
Transport length	<0.4 m
Gradient hot/cold	>~3 °C
Operation mode	Temperature regulation, on/off
Warm heat exchanger	28 x 90 x 6 mm^3
Cold heat exchanger	75 x 75 x 12 mm^3
Attachment	M4 bolts / Glue
Bus voltage	25-35 V
Power consumption	<0.3 W

Table 3. Component weight.

Component	Measured on system (g)
Pump body	36
Pump core	20
Electronics	3
Hot heat exchanger	32
Cold heat exchanger	80
Tubing, 80 cm	47
Fluid	65
Volume compensator	45
Screws etc.	4
Total	332

IV. System Specifications

The specifications have been defined to fit a specific temperature control application. This application has been chosen to show the competitiveness of the developed thermal regulation system. A specification overview is shown in Table 2. The radiator size is not specified as it is considered "outside" of the system, but for completeness, the used size was 3.2 dm^2.

The total weight of the manufactured and tested system is 332 g. A further breakdown per component is shown in Table 3. Here, an additional design iteration is expected to reduce the total weight by 10-20 % for a total weight approaching 270 g.

V. Thermal Performance

Thermal tests on the breadboard system showed the system behaves as expected. The tests were performed on a lab bench with thermocouple sensors and insulating MLI as shown in Figure 4.

A. Steady State Conductance

Initial pump on/off tests confirmed coolant pumping. This is shown in Figure 5 Left where 5W of heating is applied to the "sensor" with a room ambient at 23.5 °C. This was followed up by a constant power test with 3 W of heating for 18 h. As shown in Figure 5 Right this corresponded to a temperature difference between T_{heat} source and $T_{cold\ HX}$ of 5 °C for a thermal conductance of 0.6 W/K. The ripple shown in $T_{surrounding}$ is from the room airconditioning system. In summary the average thermal conductance was 0.59 W/K. Additional stability measurements over 24h with constant pumping power showed a stable system thermal conductance with no deviation.

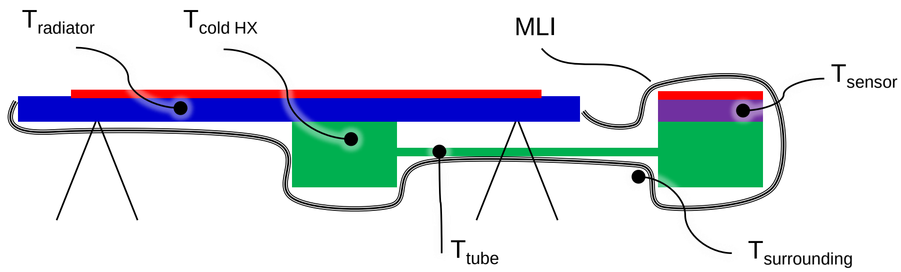

Figure 4. Lab bench test. *The system was suspended on insulating legs and wrapped in MLI prior to measurements. The thermocouple positions are indicated.*

B. Stability under Simulated Earth Albedo Heat Flux

In order to accurately measure the stability of the system under real conditions an orbital heat flux perturbation was added. This was accomplished using finite element thermal modelling of the radiator. The incoming radiation heat flux varied between 50 and 60 W/m2 over a period of 100 min, and the resulting radiator temperature function was extracted. This temperature variation was then implemented using a contact heater on the radiator in test setup.

The earth albedo heat flux perturbation and the performance of the pump regulation is shown in Figure 6. This figure also shows the room temperature $T_{surrounding}$, which shows the unfavorable regulation situation with a varying ambient temperature. The pump is regulated using a PID controller with pulse width modulation (PWM) of the on-cycle. At the black arrow the controller performs an initial auto-tune to find the correct PID parameters. At the far right in the figure another setpoint is selected with no adverse effects, only a lower duty cycle for the pump.

The max temperature variation, peak-to-peak, was 0.13 °C. This surpasses the design target of 0.15 °C even though a standard commercial of the shelf PID controller was used. Further, by removing the other disturbances

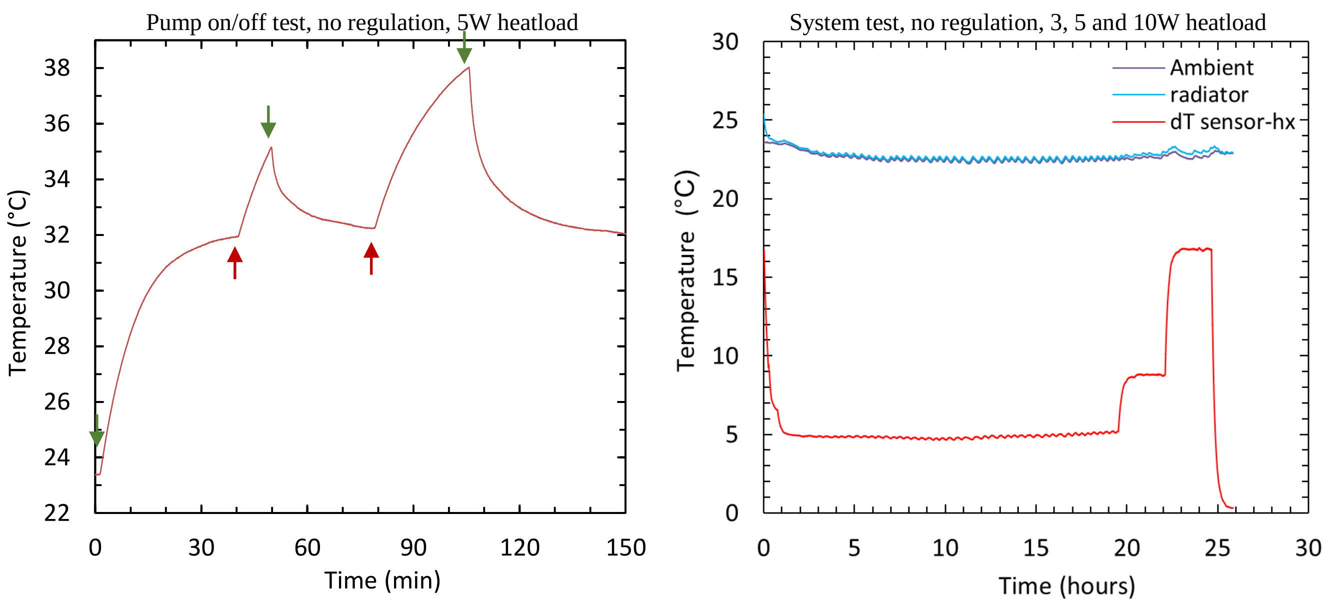

Figure 5. Left: Pump on/off test. *The pump is cycled on (green arrow) / off (red arrow) with a heat load of 5 W and a room temperature of 23.5 °C.* **Right:** *3, 5 and 10 W of heater power with the pump always on. Ripple comes from room airconditioning. The red line corresponds to the temperature difference between the sensor and the cold heat exchanger.*

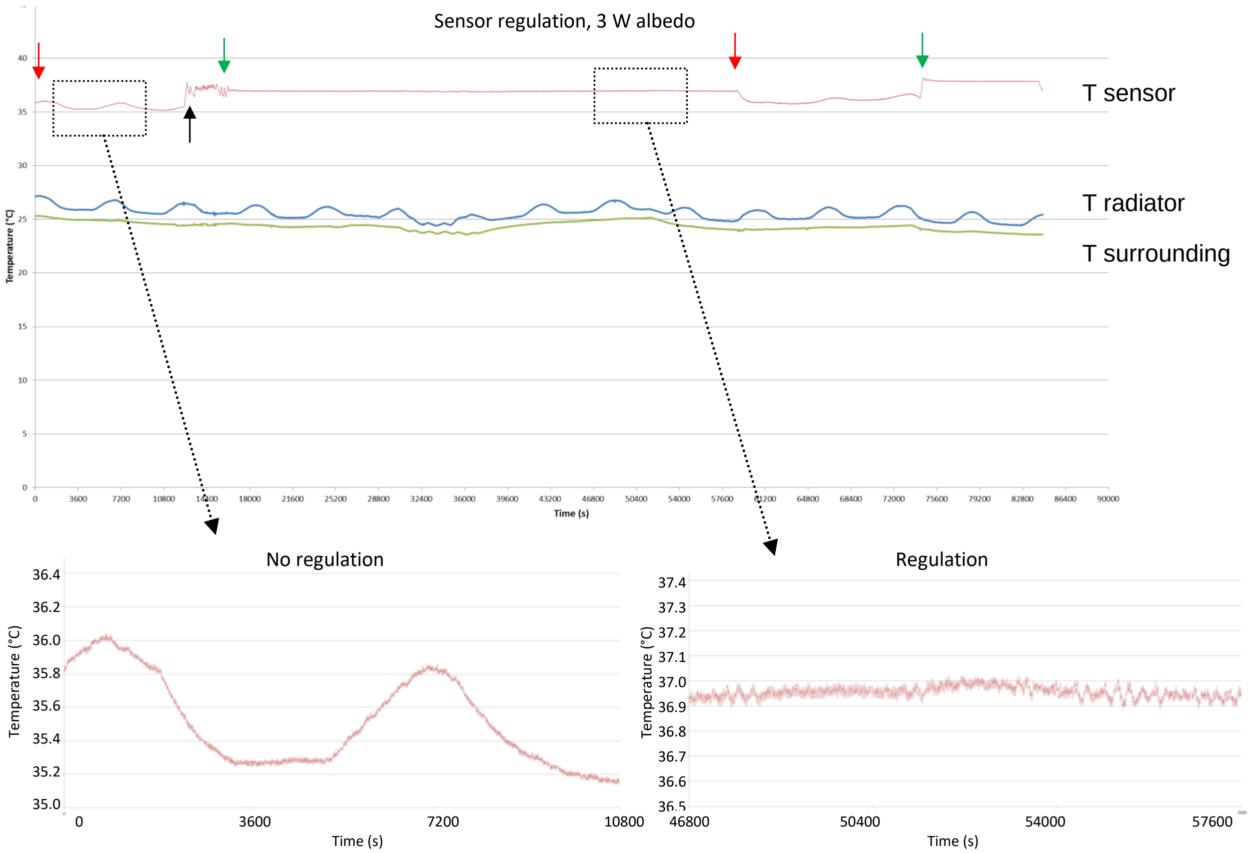

Figure 6. Heat flux perturbation and regulation. *An earth albedo heat flux variation is simulated on the radiator. This perturbation is decreased using PID control of the pump (PWM). Red and green arrows indicate off and on for the regulation while the black arrows shows the PID auto-tune.*

caused by the surrounding air even better performance is expected when tested in a chamber under thermal vacuum. Finally, it should be noted that this regulation does not in any way use added heat for regulation, only the variable conductance of the mass flow is used for temperature control.

VI. Reduced thermal mathematical model

The heat exchangers transfer the heat flow from the dissipating equipment to the liquid and from the liquid to the radiators or cold plate. There are two thermal conductances involved in this process (1) thermal conduction in the

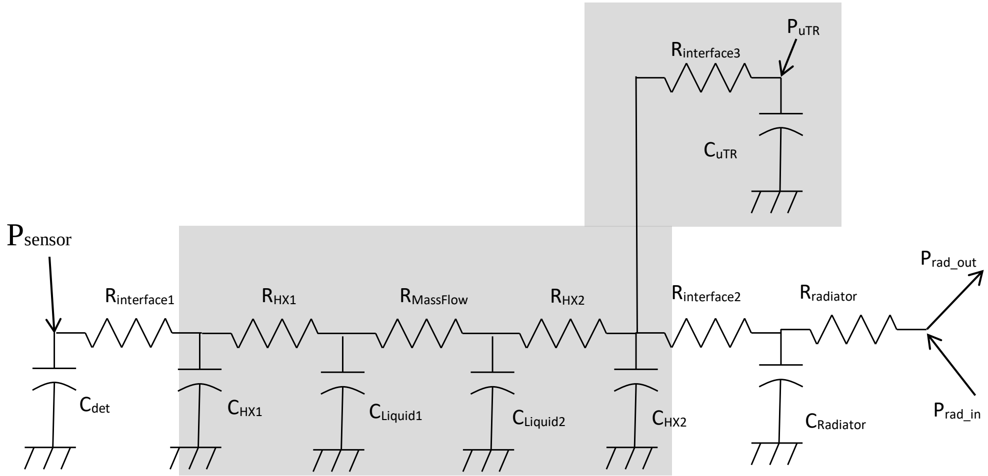

Figure 7. Reduced thermal mathematical model. *The developed system is within the marked area.*

Table 4. The elements of the thermal model.

Element	Physical description	Value
$R_{interface1}$	Thermal resistance of the interface between the sensor and the heat exchanger.	0.20 K/W
R_{HX1}	Thermal resistance from the surface of the heat exchanger to the liquid. Internal thermal conduction and internal surface to liquid heat transfer.	0.22 K/W
$R_{MassFlow}$	Representative thermal conduction of the mass flow and corresponding heat flow between the heat exchangers. Depends on the liquid flow rate and the specific thermal capacity of the liquid.	0.59 W/K
R_{HX2}	Same as for R_{HX1}, but radiator side and aluminum not Shapal	0.11 K/W
$R_{interface2}$	Thermal resistance of the interface between the heat exchanger and the radiator.	0.090 K/W
$R_{radiator}$	Thermal resistance through the radiator, 3.2 dm^2 area	0.28 K/W

structural part of the heat exchanger and (2) forced convection heat transfer from the internal surface of the heat exchanger to the liquid. The thermal conduction is determined by the thermal conductivity of the material and the geometrical design of the heat exchanger. The convection heat transfer, normally the most important, is determined by the heat transfer coefficient. Due to predominantly laminar flow conditions the so-called Nusselt number is more or less constant and the only way to improve the solid to liquid heat transfer is the width of the channels inside the heat exchangers. Furthermore the total wetted surface is also important. The design of the heat exchanger should maximize the internal wetted surface area in order to maximize the thermal conductance. The same considerations applies to both the cold side and hot side heat exchangers.

The heat transfer from the liquid at the hot side heat exchanger to the liquid at the cold side heat exchanger is a mass transfer and the thermal conductance is basically proportional to the liquid flow rate times the specific heat capacity and the density of the liquid.

The model presented in Figure 7 omits any environmental interactions. This is because vacuum testing has not been performed so far and the environmental interactions are more difficult to accurately model. The values of the model is assembled from a limited set of measurement thus not all parameters in Table 4 can be extracted only based on experimental data. The total thermal resistance has been confirmed by measurement.

VII. Electronics

The proposed circuit design for the system is a boost converter circuit followed by a diode multiplier, shown in Figure 8.

The boost converter creates an alternating voltage from the DC input voltage. The voltage is increased from the input bus voltage 25-35 V to around 100-150 V AC by an inductor. This is a suitable input voltage to the diode multiplier and still sufficient low to not impose very high voltage stress to any individual component.

The basic voltage multiplier is constructed from diodes and capacitors only. On the board, the diode voltage pump is located on the right side. The 30 V input connection is located on the left side and the high voltage connections is on the right side.

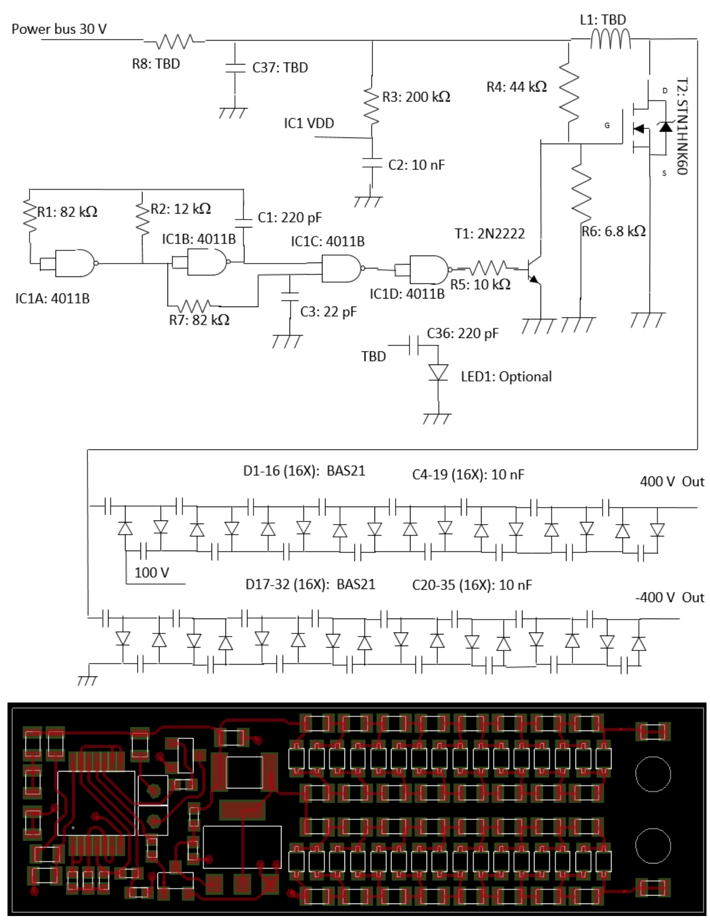

Figure 8. Electronics schematic above and PCB layout below

The main advantages of the diode voltage multiplier circuit are; (1) simple circuit and low cost components, (2) the circuit is inherently a voltage divider and no single component need to withstand the total voltage potential and (3) no inductive components needed. Drawbacks are; (1) switching noise may be a problem, (2) limited current capability although no major issue for EHD and (3) limited efficiency. The power supply PCB was designed in conformance with ECSS Q ST 70 12C although it covers only voltages up to 500 V. The components selected are either listed in the ESCC EPPL or equivalent to EPPL parts.

VIII. Conclusion

The development and performance of a miniature pumped fluid loop for thermal regulation has been presented. The shown thermal control is suitable for a wide range of applications and the systems thermal envelope is adaptable.

Acknowledgments

This work was in part sponsored by the Swedish National Space Board.

References

[1]Castellanos, A., *Electrohydrodynamics*, CISM International Centre for Mechanical Sciences Series, Springer-Verlag, Wien, 1998.

[2]Seyed-Yagoobi, J., “Electrohydrodynamic pumping of dielectric liquids”, *Journal of Electrostatics*, Vol. 63, No. 6-10, June 2005, pp. 861-869.

[3]Thorslund, R, Björneklett, A, Antelius, M, Tjiptahardja, T, Huens, T, Scommegna, A, Walker, A, “Development of an Engineering Model of a monophasic Electro Hydro Dynamic (EHD) pumped fluid loop within the frame of the NEOSAT pre-development activities” *46th International Conference on Environmental Systems*, Vienna, Austria, 2016, pp. 436

[4]Pearson, M., “Micro-scale EHD conduction-driven pumping and heat transfer enhancement in single- and two-phase systems”, PhD. Dissertation, Illinois Institute of Technology, Chicago, 2011.

[5]Pearson M. R., , Seyed-Yagoobi, J., “Experimental study of EHD conduction pumping at the meso- and micro-scale”, Journal of Electrostatics, Vol. 69, No. 6, Dec 2011, pp. 479-485.

[6]Patel, V.K., Robinson, F., Seyed-Yagoobi, J., and Didion, J., "Terrestrial and Microgravity Experimental Study of Microscale Heat-Transport Device Driven by Electrohydrodynamic Conduction Pumping", IEEE Transactions on Industry Applications, Vol. 49, No. 6, pp. 2397-2401, Nov.-Dec. 2013.